Application of a temperature-dependent liquid-drop model to dynamical Langevin calculations of fission-fragment distributions of excited nuclei

E. G. Ryabov,[1] A. V. Karpov,[2] P. N. Nadtochy,[1] and G. D. Adeev[1]
[1]*Omsk State University, Prospect Mira 55-A, RU-644077, Omsk, Russia*
[2]*Flerov Laboratory of Nuclear Reactions, Joint Institute for Nuclear Research, Dubna RU-141980, Russia*
(Received 1 April 2008; published 16 October 2008)

A stochastic approach to fission dynamics based on three-dimensional Langevin equations was applied to calculation of the mass-energy and angular distributions of fission fragments. The dependence of the mass-energy distribution parameters on the angular momentum and the anisotropy of the fission-fragment angular distribution on excitation energy have been studied in a wide range of the fissility parameter. A temperature-dependent finite-range liquid-drop model was used in a consistent way to calculate the functional of the Helmholtz free energy and level-density parameter. The modified one-body mechanism of nuclear dissipation (the so-called surface-plus-window dissipation) was used to determine the dissipative forces in Langevin equations. The evaporation of light prescission particles was taken into account on the basis of a statistical model combined with Langevin dynamics. The calculated parameters of the mass-energy distribution and their angular dependencies are in good quantitative agreement with the available experimental data at the value of the reduction coefficient of the contribution from the wall formula equal to 0.25. Analysis of the anisotropy of the fission-fragment angular distribution performed with the saddle-point transition state model and scission-point transition state model indicates that it is necessary to take into account the dynamical aspects of the fission-fragment angular distribution formation.

DOI: 10.1103/PhysRevC.78.044614 PACS number(s): 25.85.−w, 05.10.Gg

I. INTRODUCTION

Formation of the fission-fragment distributions is a very complicated process. To describe theoretically this process one must solve several important problems. For instance, one has to decide how shell structure is reorganized with excitation energy and deformation and how to relate collective and internal degrees of freedom of nucleus. The later relation is often treated and modeled as a nuclear viscosity. For a nucleus with a high excitation energy the situation simplifies. Theoretical investigations [1,2] and experimental analysis of the fission-fragment mass-energy distribution at low and medium excitation energies [3] demonstrated that the shell effects can be neglected for nucleus with excitation energy above 50 MeV, so the nucleus can be considered as a charged liquid drop.

The liquid-drop model (LDM) predicts the symmetric energy and mass distributions of fission fragments for hot heavy nuclei [4,5]. The theoretical assumption on predominantly symmetric fission of hot nuclei is confirmed by many experiments [3,6]. The compound nuclei formed in heavy-ion fusion reactions can have an angular momentum l in a large interval from 0 to $l_{\max}$, where $l_{\max}$ is angular momentum at which fission barrier of the nucleus is vanished. Therefore, the question about the influence of angular momentum on the characteristics of the mass-energy distribution (MED) of fission fragments is very important for the investigation in fusion-fission reactions.

The finite-range LDM based on the Yukawa-plus-exponential potential was formulated and developed at the end of the 1970s in pioneering works [7–9]. During the last two decades it has been extensively and rather successfully employed to calculate various properties of nuclei [10–13]. However, it should be stressed that the most part of applications of the finite-range LDM is restricted to nuclei at zero temperature. For this case, a standard set of data consisting of all empirically known ground-state binding energies and fission barrier heights (corrected for shell and deformation effects), some fusion barrier heights, equivalent shape radii, and the average charge diffuseness are used for fitting the parameters of the finite-range LDM providing high accuracy in nuclear structure calculations [10,11,13]. Obviously, such an experimental information does not exist for hot nuclei. Therefore, one has to rely on some theoretical approach, for instance, the extended temperature-dependent Thomas-Fermi calculations [14]. A few years ago the finite-rage LDM based on the Yukawa-plus-exponential potential has been generalized by Krappe [15] to describe the temperature dependence of the nuclear free energy. This dependence is obtained by fitting the results of the former temperature-dependent Thomas-Fermi calculations [16] with a finite-range mass formula.

Experimental investigations of the MED dependence on l were carried out more than 10 years ago. Obtained results are summarized in works of Itkis, Rusanov, Chubaryan, and coworkers [17–19] for a wide range of fissility parameter. The analysis of the mass distribution dependence on l has shown that fissioning nuclei can be divided into two groups. For the first group ($Z^2/A \geqslant 31$) the variance of the mass distribution σ_M^2 increases as the angular momentum of the compound nucleus becomes larger, i.e., $d\sigma_M^2/dl^2 > 0$. For the second group (light fissioning nuclei with $Z^2/A < 30$) the mass distribution variance decreases as the angular momentum increases, i.e., $d\sigma_M^2/dl^2 < 0$. For the nuclei in the range of fissility between these two cases, for example, Pt and Os, $d\sigma_M^2/dl^2 \simeq 0$.

The mean kinetic energy of fission fragments $\langle E_K \rangle$ depends slightly on l with maximum value for the dependence coefficient $d\langle E_K \rangle / dl^2 = 0.3\,\mathrm{keV}/\hbar^2$ [18,19]. The variance of the kinetic energy distribution of fission fragments $\sigma^2_{E_K}$ is independent of the angular momentum for the light fissioning nuclei, whereas for the medium and heavy nuclei the derivative $(d\sigma^2_{E_K}/dl^2 > 0)$ is positive but small.

The theoretical aspects of the influence of the angular momentum on the fission-fragment mass-energy distribution were considered in many works (see Ref. [18] and references therein). However, their results are often contradict each other and investigations are performed for one or two compound systems only. Nevertheless, we should mention here works of Gregoire and Scheuter [20], Faber [21], and Glagola *et al.* [22]. In spite of the fact that the experimental data, sketched above, were published more than 10 years ago, theoretical works of Adeev *et al.* [23,24] are the ones of a few full-scale investigations of the l dependence of the MED until our recent and present works. The investigations of the MED dependence on l made by Adeev with coworkers [23,24] report qualitative agreement with conclusions of the above summarized analysis of Itkis *et al.* [18,19]. Although the values of the derivative $d\sigma^2_M/dl^2$ are underestimated in comparison with the experimental results [18,19], the main features of the $d\sigma^2_M/dl^2$ dependence on the fissility Z^2/A are reproduced.

Many recent works have demonstrated the successful application of the multidimensional Langevin equations to the fission of excited compound nuclei formed in reactions induced by heavy ions [25–31]. From the physical point of view, the Langevin equations are equivalent to the Fokker-Planck equation, which was widely used for modeling the fission of excited nuclei in the framework of the diffusion model [23,24]. Particularly, the calculations of the MED characteristics by Adeev *et al.* [23,24] were made by means of the Fokker-Planck equation. The multidimensional Langevin equations are more suitable for computer modeling. A very important feature of our model based on the Langevin equations [25,26] is the possibility to take into account particles evaporation via combining the dynamical model with the statistical one, as it was proposed by Mavlitov, Fröbrich, and Gontchar [32,33]. Thus, our combined dynamical-statistical model allows us to describe the MED parameters with emission of the light particles and γ quanta. This model allows one to estimate temperature at scission more precisely, which, according to our results, is very important in the case of the MED parameters investigations.

We investigated in detail the l dependence of the mass distribution in Ref. [34] and the dependence of $d\sigma^2_M/dl^2$ on l was considered in detail. In the present work we generalize the former results and pay our attention mostly to the l dependences of the MED parameters. We investigate also the angular distribution of fission fragments within the standard transition-state theory [35]. The essence of this model consists in the assumption that there is a certain chosen (transition) configuration of a fissioning system that determines the angular distribution of fission fragments. Usually there are two limiting assumptions on the position of the transition state and, correspondingly, two variants of the transition-state theory: the saddle-point transition-state (SPTS) [35] model and the scission-point transition-state model (SCTS) [36]. In addition to the angular distribution, the same assumptions are often used in theoretical and experimental analysis of the MED characteristics [19]. So our investigations were dealt with the similar theoretical ideas about the process of formation of various fission-fragment distributions.

The article is organized as follows: to make the article self-contained we describe in Sec. II the model [26–29,34,37] with some technical aspects and details. Section III is devoted to the discussion of the calculated results and comparison with available experimental data. Finally, in Sec. IV, the concluding remarks are given.

II. THE MODEL

The three-dimensional Langevin model with input parameters has been presented and discussed in detail in previous publications [26–29,34]; therefore, only the key features and formulas are described here.

A. Dynamical Langevin equations

In the dynamical calculations we applied the $\{c, h, \alpha\}$ parametrization [38]. In cylindrical coordinates the surface of the nucleus is given by:

$$\rho_s^2(z) = \begin{cases} (c^2 - z^2)\left(A_s + Bz^2/c^2 + \frac{\alpha z}{c}\right), & B \geqslant 0; \\ (c^2 - z^2)\left(A_s + \frac{\alpha z}{c}\right)\exp(Bcz^2), & B < 0, \end{cases} \tag{1}$$

where z is the coordinate along the symmetry axis and ρ_s is the radial coordinate of the nuclear surface. In Eq. (1) the quantities B and A_s are defined by:

$$\begin{aligned} B &= 2h + \frac{c-1}{2}; \\ A_s &= \begin{cases} c^{-3} - \frac{B}{5}, & B \geqslant 0; \\ -\frac{4}{3}\frac{B}{\exp(Bc^3) + \left(1 + \frac{1}{2Bc^3}\right)\sqrt{-\pi Bc^3}\,\mathrm{erf}\left(\sqrt{-Bc^3}\right)}, & B < 0. \end{cases} \end{aligned} \tag{2}$$

In Eqs. (1) and (2), c denotes the elongation parameter, the parameter h describes the variation in the thickness of the neck for a given elongation of the nucleus, and the parameter of the mass asymmetry α determines the ratio of the volumes of the future fission fragments.

The coupled Langevin equations have the form:

$$\begin{aligned} \frac{dq_i}{dt} &= \mu_{ij} p_j, \\ \frac{dp_i}{dt} &= -\frac{1}{2} p_j p_k \frac{\partial \mu_{jk}}{\partial q_i} + Q_i - \gamma_{ij}\mu_{jk} p_k + \theta_{ij}\xi_j(t), \end{aligned} \tag{3}$$

where $\mathbf{q}$ is the vector of collective coordinates, $\mathbf{p}$ is the vector of conjugate momenta, Q_i is the driving force, $m_{ij}(\mathbf{q})$ $(\|\mu_{ij}\| = \|m_{ij}\|^{-1})$ is the tensor of inertia, and $\gamma_{ij}(\mathbf{q})$ is the friction tensor. The normalized random variable $\xi_j(t)$ is assumed to be white noise. The strength of the random force θ_{ij} is given by $\sum \theta_{ik}\theta_{kj} = T\gamma_{ij}$. The temperature of the "heat bath" T is determined by the Fermi-gas model formula $T = [E_{\mathrm{int}}/a(\mathbf{q})]^{1/2}$, where E_{int} is the internal excitation energy of the nucleus and $a(\mathbf{q})$ is the level-density parameter. It is calculated in the framework of temperature-dependent

finite-range liquid-drop model, formulated by Krappe [15]. The repeated indices in the equations above imply summation over the collective coordinates. The method for calculation of the level-density parameter $a(\mathbf{q})$, the Helmholtz free energy $F(\mathbf{q})$, the potential energy of the nucleus $V(\mathbf{q})$, and the driving force $Q(\mathbf{q})$, entering the Langevin equations (3) is considered particularly in the next subsection.

In Ref. [27] we introduced a new mass-asymmetry parameter scaled with elongation $\alpha' = \alpha c^3$, which has the same meaning as α. Hence, we used $\mathbf{q} = (c, h, \alpha')$ as collective coordinates in our modeling. During a random walk along the Langevin trajectory in the space of the collective coordinates, the energy conservation law is used in the form $E^* = E_{\rm int} + E_{\rm coll} + V + E_{\rm evap}(t)$. Here E^* is the total excitation energy of the nucleus, $E_{\rm coll} = 1/2 \sum \mu_{ij} p_i p_j$ is the kinetic energy of the collective degrees of freedom, V is the potential energy of the nucleus, and $E_{\rm evap}(t)$ is the energy carried away by evaporated particles by the time t.

The inertia tensor is calculated by means of the Werner-Wheeler approximation for incompressible irrotational flow [39]. A modified one-body mechanism of nuclear dissipation [40,41] is used to determine the dissipative part of the driving forces. The expression applied to calculate the friction tensor for the so-called surface-plus-window dissipation can be found in our previous works [27,28]. We use the reduction coefficient of the contribution from the wall formula equal to 0.25. This value is very close to the one extracted from experimental analysis [40] on the widths of giant resonances (0.27). Our previous calculations [27,28] showed that the experimental data on the mean prescission neutron multiplicities and MED variances can be reproduced with the reduction coefficient in the range 0.25–0.5.

We start modeling the fission process from the spherical compound nucleus assuming that the intrinsic degrees of freedom are thermalized and the thermal equlibrium momentum distribution is established. This choice of the initial conditions means that we restrict ourselves to a situation where an equilibrated compound nucleus has been formed in a heavy-ion fusion reaction before the fission process starts. The most part of the calculations were done for the fixed initial angular momentum l. The fission fragment angular distribution was investigated with the spin distribution $d\sigma(l)/dl$ for heavy-ion complete fusion. We have parameterized the compound nuclei spin distribution $d\sigma(l)/dl$ according to the scaled prescription [42,43], which reproduces to a certain extent the dynamical results of the surface friction model [44] for fusion of two heavy ions.

Evaporation of the prescission light particles ($j = n, p, \alpha, \gamma$) along the Langevin fission trajectories is taken into account using a Monte Carlo simulation technique [32,42]. All dimensional factors were recalculated when a light prescission particle was evaporated; only dimensionless functionals of the rotational, Coulomb, and nuclear energies were not recalculated. This procedure provides a good accuracy in calculating the potential and the Helmholtz free energies. The loss of the angular momentum was taken into account by assuming that the light particles carry away $l_j = 1, 1, 2, 1$ [42]. In other words, we recalculate the potential energy, the level-density parameter (see our previous work, Ref. [29], for details) and the factors for the inertia and viscosity tensors after each evaporation event. These computations are obligatory, because the evaporation of light particles results in a change of the nucleonic composition of the initial nucleus.

In the present work we studied few compound nuclei with a rather low fissility (especially for the ^{162}Yb nucleus). This was possible only by switching over to a statistical model description with a Kramers-type fission decay width after delay time, when stationary flux over the saddle point is reached. This procedure was first proposed in Ref. [32] and successfully used in our previous works. Main features and formula can be found in Ref. [34].

B. Generalized temperature-dependent finite-range liquid-drop model

In the dynamical description of fission within Langevin dynamics one of the important question is to determine the driving force Q_i, which governs the collective motion of the nuclear system. As it was stressed by Fröbrich [45] and McCalla and Lestone [46] the driving force of a hot system is not a simply the negative gradient of the conservative potential but should contain a thermodynamical correction. This statement was proved clearly in Ref. [45]. Nevertheless, there are several recent works that use bare potential energy instead of some thermodynamic potential to calculate the driving force of a hot nuclear system [31,47].

We employed a Helmholtz free energy calculated within generalized temperature-dependent LDM with the finite range of nuclear forces, formulated by Krappe [15] to get the driving force for the hot nuclei. Here we introduce the notion temperature-dependent finite-range LDM (temperature-dependent FRLDM) in contrast to LDM [1,48].

The free Helmholtz energy in the temperature-dependent FRLDM based on the Yukawa-plus-exponential mass formula as a function of the mass number $A = N + Z$, relative neutron excess $I = (N - Z)/A$, the temperature, the angular momentum, and a set of collective coordinates $\mathbf{q}$ has been suggested [15] in the following form:

$$\begin{aligned} F(A, Z, \mathbf{q}, T, l) &= -a_v(1 - k_v I^2)A + a_s(1 - k_s I^2)B_n(\mathbf{q})A^{2/3} + c_0 A^0 \\ &\quad + a_c \frac{Z^2}{A^{1/3}} B_c(\mathbf{q}) - a_c \frac{5}{4}\left(\frac{3}{2\pi}\right)^{2/3} \frac{Z^{4/3}}{A^{1/3}} + \frac{\hbar^2 l(l+1)}{2J(\mathbf{q})}, \end{aligned} \quad (4)$$

where a_v, a_s, and a_c are the usual volume, surface, and Coulomb energy parameters of the temperature-dependent FRLDM at zero temperature and k_v and k_s are the corresponding volume and surface asymmetry parameters. The shape functions in Eq. (4): $B_n(\mathbf{q})$, $B_c(\mathbf{q})$, and $J(\mathbf{q})$ are the functionals of the generalized nuclear energy, the Coulomb energy, and the rigid-body moment of inertia, which takes into account the diffuseness of a realistic nuclear density [49]. The last term in Eq. (4) represents the rotational energy of the nucleus. The functionals $B_n(\mathbf{q})$, $B_c(\mathbf{q})$, and $J(\mathbf{q})$ take into account the finite range of the nuclear forces and the diffusiness of nuclear matter and charge distributions using the parameters a, a_M, and a_d, respectively.

Equations for $B_n(\mathbf{q})$, $B_c(\mathbf{q})$ can be found in Ref. [34]. The rigid-body moment of inertia $J(\mathbf{q})$ is defined as follows [10]:

$$J(\mathbf{q}) = J_0 \left[J_{\max} + 10 \left(\frac{a_M}{R_0} \right)^2 \right], \tag{5}$$

where $J_0 = \frac{2}{5} M_0 R_0^2$ is the rigid-body moment of inertia for the spherical nucleus with the mass $M_0 = m_0 A$ and $R_0 = r_0 A^{1/3}$ is the radius of the spherical nucleus. The diffuseness parameter for matter distribution a_M is assumed to be equal to the diffuseness parameter of the charge distribution, i.e., $a_M = a_d$ [10].

$$J_{\max} = \begin{cases} J_\perp, & \text{if} \quad J_\perp > J_\parallel, \\ J_\parallel, & \text{if} \quad J_\perp < J_\parallel, \end{cases} \tag{6}$$

where $J_\parallel = \frac{15}{16} \int_{z_{\min}}^{z_{\max}} dz\, \rho_s^4$, $J_\perp = \frac{15}{32} \int_{z_{\min}}^{z_{\max}} dz\, \rho_s^2 (4z^2 + \rho_s^2)$ are the rigid body moments of inertia at deformation $\mathbf{q}$ in units of J_0 with respect to the symmetry axis and to the axis perpendicular to the symmetry axis, respectively; $z_{\min}$ and $z_{\max}$ are the left and right ends of the nuclear surface.

The temperature dependence of the seven coefficients entering equation (4) a_v, a_s, k_v, k_s, r_0, a, and a_d is parameterized in the form

$$a_j(T) = a_j(T = 0)(1 - x_j T^2), \tag{7}$$

that is expected [16] to be valid for $T \leqslant 4$ MeV. The most complete information about the thermal coefficients x_j has been obtained through the self-consistent extended Thomas-Fermi calculations with SkM* interaction [14,16]. A liquid-drop expansion of these results for the Gibbs free energy was converted to the structure of Eq. (4) in Ref. [15]. The values of 14 parameters recommended in Ref. [15] and used in the present work can be found in Table I.

If the Helmholtz free energy is available, the entropy and the level-density parameter can be obtained from thermodynamic relation and well-known formula of the Fermi-gas model

$$S(\mathbf{q}, T) = -\left[\frac{\partial F(\mathbf{q}, T)}{\partial T} \right]_V, \quad a(\mathbf{q}, T) = \frac{S(\mathbf{q}, T)}{2T}. \tag{8}$$

A valuable conclusion was made in Ref. [29]: $a(\mathbf{q}, T)$ is weakly dependent on the nuclear temperature T. Thus, we suppose $a(\mathbf{q}, T)$ in the temperature-dependent FRLDM being independent of the T and calculation of $a(\mathbf{q}, T)$ has been performed at $T = 1.5$ MeV. It appreciably simplifies application of the temperature-dependent FRLDM, especially, in the multidimensional Langevin simulations.

TABLE I. The temperature-dependent FRLDM coefficients. Values at zero temperature (the first row) and temperature coefficients x_j in MeV^{-2} (the second row).

	r_0 (fm)	a (fm)	a_d (fm)	a_v (MeV)	k_v	a_s (MeV)	k_s
$a_j(0)$	1.16	0.68	0.7	16.0	1.911	21.13	2.3
$10^3 x_j$	0.736	7.37	7.37	3.22	5.61	4.81	14.79

Deformation dependence of the level-density parameter is often approximated by

$$a(\mathbf{q}) = a_1 A + a_2 A^{2/3} B_s(\mathbf{q}), \tag{9}$$

where $B_s(\mathbf{q})$ is the dimensionless functional of the surface energy in the LDM with a sharp surface [38] and a_1 and a_2 are the volume and surface coefficients of the level-density parameter. In dynamical modeling the two sets of the coefficients a_1 and a_2 are frequently used [50,51]. Ignatyuk and coworkers proposed $a_1 = 0.073\,\text{MeV}^{-1}$ and $a_2 = 0.095\,\text{MeV}^{-1}$, whereas the coefficients of Töke and Swiatecki are $a_1 = 0.0685\,\text{MeV}^{-1}$ and $a_2 = 0.274\,\text{MeV}^{-1}$. It was shown in our works [29,34], that the level-density parameter from the temperature-dependent FRLDM [15] is close to the values of $a(\mathbf{q})$ in the Ignatyuk parametrization, regardless of the dependence one examines: deformation dependence of $a(\mathbf{q})$ for a given nucleus or a fissility parameter dependence of $a(\mathbf{q})$ for the spherical nuclei. This fact can be explained by the results of our approximation, made in Ref. [29]. We carried out an approximation procedure of the $a(\mathbf{q})$ deformation dependence by expression (9) to estimate the values of the coefficients a_1 and a_2. The estimated values are $a_1 = 0.0598$ MeV^{-1} and $a_2 = 0.1218$ MeV^{-1}. The coefficient a_1 has close values in all mentioned approximations of $a(\mathbf{q})$, whereas the value of a_2 estimated in Ref. [29] is quite close to the Ignatyuk coefficient and differs more than twice from the value of Töke and Swiatecki. In the Langevin calculations we used the exactly calculated level-density parameter, obtained from Eqs. (8).

From the Fermi-gas model one has

$$E_{\text{int}}(\mathbf{q}, T) = a(\mathbf{q}) T^2, \tag{10}$$

and

$$F(\mathbf{q}, T) = V(\mathbf{q}) - a(\mathbf{q}) T^2, \tag{11}$$

where $V(\mathbf{q})$ is the zero-temperature potential energy $[F(\mathbf{q}, T = 0) \equiv V(\mathbf{q})]$. The microscopic self-consistent Thomas-Fermi calculations with SkM* interaction [14] have shown that equation (11) can be a reasonable approximation for $T \leqslant 4$ MeV.

The expressions for the driving force Q read as follows [45]:

$$Q_i(\mathbf{q}) = \left(T \frac{dS}{dq_i} \right)_{E^* = \text{const}}$$

or

$$Q_i(\mathbf{q}) = -\left[dF(\mathbf{q})/dq_i \right]_{T = \text{const}}. \tag{12}$$

It should be noted that both definitions of $Q_i(\mathbf{q})$ are equivalent in the case of the strong nuclear viscosity [52]. It is evident from Eqs. (11) and (12) that the driving force in the Langevin equations can be evaluated easily within the temperature-dependent FRLDM:

$$Q_i(\mathbf{q}) = -\left[\frac{dV}{dq_i} - \frac{da(\mathbf{q})}{dq_i} T^2 \right]_{T = \text{const}}.$$

As a result, in the framework of the temperature-dependent FRLDM one can calculate consistently the two main input parameters of the Langevin simulations combined with the statistical model: the driving force and the level-density

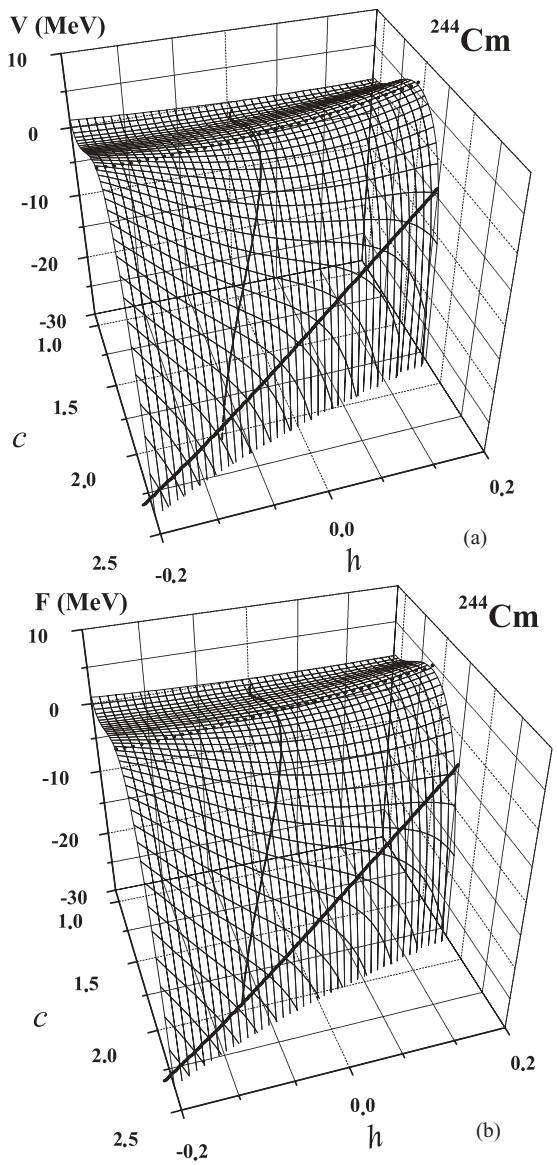

FIG. 1. The potential energy surface (a) and the free energy surface (b) for the compound nucleus ^{244}Cm at $\alpha' = 0$ and zero angular momentum. The thin solid curves are the mean dynamical trajectories. The thick lines are the scission line determined from the intersection of the scission surface (see text for explanation) and the plane $\alpha' = 0$. The dotted line is the ridge line. The mean dynamical trajectories were calculated with the reduction coefficient value 0.25.

parameter. The zero-temperature potential energy $V(\mathbf{q})$, which enters Eq. (11), can be calculated also within the finite-range model with the Sierk coefficients [10], as the values of coefficients a_j at zero temperature, presented in the first row of Table I, are equal to the coefficients obtained by Sierk in Ref. [10].

Figure 1 illustrates explicitly the difference between the potential energy map (free energy at zero temperature) and free energy at temperature $T = 2$ MeV for the compound nucleus ^{244}Cm. Fission barriers for these two cases are 3.35 and 2.21 MeV, correspondingly. The mean Langevin trajectory [27] and the scission line are also presented in Fig. 1 to illustrate the physics of fission process within the Langevin dynamics.

Concluding the description of the temperature-dependent FRLDM we would like to recall that suggestion to take into account temperature effects in the LDM of nuclear fission was done by Hasse and Stocker [53,54] three and a half decades ago. Their temperature-dependent LDM with a sharp surface was based on a Thomas-Fermi description of the excited nucleus and contained two temperature-dependent parameters: the surface tension and the nuclear density. The temperature dependence of the both parameters was assumed similar to Eq. (7). In the well-known calculations [25,55] the temperature dependence of the generalized surface energy was included in the form $E_s(q, T) = E_s(q, T = 0)(1 - \xi T^2)$. The parameter ξ was calculated with the extended Thomas-Fermi model [56]. Dynamical Langevin calculations in Ref. [55] were carried out with two values of $\xi (\xi = 0.014$ MeV^{-2} and $\xi = 0.009$ MeV^{-2}) and with the Töke and Swiatecki level-density parameter. The conservative force in Ref. [55] was calculated as the derivative of the temperature-dependent potential energy. It is easy to see that using such a temperature-dependent potential is equivalent to using the Helmgoltz free energy for calculating of the driving force of a thermodynamical system. Use of the temperature-dependent term in surface energy is not fully satisfactory from the point of view of consistency of model, in spite of a good agreement between calculated results and experimental data in Refs. [25,55].

To calculate observables we should introduce a notion for the nucleus scission configuration. It is determined by the intersection point of the stochastic Langevin trajectory of the fissioning system with the scission surface in the coordinate subspace. It has been supposed that the scission occurred when the neck radius of the fissioning nucleus R_N was equal to $0.3R_0$ [38,57]. This scission condition determines the scission surface in the space of the collective coordinates. The value $R_N = 0.3R_0$ for scission configuration was defined on the basis of the criterion of instability of a nucleus against variations in the thickness of its neck [38]. It was shown in Ref. [58] that a choice of the scission criterion is a more crucial only in the case of studying the energy distribution characteristics, but, nevertheless, there is no certain answer for which scission criterion should be used [58]. It is assumed that the distribution of collective variables and momenta are formed during the descent from the saddle to the scission configuration, where the neck nucleus ruptures immediately without extra elongation. The influence of further evolution of the collective variables on the fission-fragment distributions is neglected. Previously, this assumption was also used in the MED investigations within the diffusion model with the Fokker-Plank equation.

It was assumed in calculations of the energy distribution parameters that the total kinetic energy E_K of fission fragments is the sum of the Coulomb repulsion energy V_c, the nuclear attraction energy V_n of the nascent fragments, the kinetic energy of their relative motion (prescission kinetic energy $E_{\rm ps}$), and fission-fragment relative rotational energy $V_{\rm rot}$. All parts of this sum are calculated at the moment of scission. The mean value of the total kinetic energy $\langle E_K \rangle$ is found as

$$\langle E_K \rangle = \langle V_c \rangle + \langle V_n \rangle + \langle E_{\rm ps} \rangle + \langle V_{\rm rot} \rangle, \qquad (13)$$

and its variance was found according to

$$\sigma^2_{E_K} = \langle E_K^2 \rangle - \langle E_K \rangle^2 . \quad (14)$$

Here and further in this article the angular brackets denote averaging over an ensemble of the stochastic Langevin trajectories. We have calculated V_c and V_n within temperature-dependent FRLDM. Explicit formulas can be found in Refs. [15,29,34,37].

The relative rotational energy of fragments $V_{\rm rot}$ is calculated by the expression, suggested by Carjan and Kaplan [59]

$$V_{\rm rot} = \left[\frac{\mu D^2}{(J_1 + J_2 + \mu D^2)}\right]\left[\frac{\hbar^2 l(l+1)}{2(J_1 + J_2 + \mu D^2)}\right], \quad (15)$$

where J_1 and J_2 are the moments of inertia calculated for spherical fission fragments, μ is the reduced mass, D is the distance between centers-of-mass of fission fragments, and l is the angular momentum for the compound nuclei. Here we neglect the spins of projectile and target nucleus and assume that the full moment of the system $I \simeq l$. It should be noted that an equation similar to Eq. (15) was used in Ref. [60] to take into account energy of the relative rotation of the fission fragments to calculate the total kinetic energy of the fission fragments for binary fission of the light nuclei.

The mass of fission fragments was calculated according to:

$$M_R = \frac{A\int_{z_N}^{z_{\max}} \rho_s^2(z, \mathbf{q}_{\rm sc})dz}{\int_{z_{\min}}^{z_{\max}} \rho_s^2(z, \mathbf{q}_{\rm sc})dz}, \quad M_L = \frac{A\int_{z_{\min}}^{z_N} \rho_s^2(z, \mathbf{q}_{\rm sc})dz}{\int_{z_{\min}}^{z_{\max}} \rho_s^2(z, \mathbf{q}_{\rm sc})dz}, \quad (16)$$

where A is the mass of the nucleus, corrected for the particles evaporation prior scission; M_R and M_L are the mass of the right and left fission fragment; $\mathbf{q}_{\rm sc}$ is the scission configuration of the nucleus; $z_{\min}$ and $z_{\max}$ are the left and right ends of the nuclear surface; and z_N is the position of the neck plane that divides the nucleus into two parts. We have chosen the position of the z_N at the minimum of $\rho_s^2(z)$.

III. RESULTS AND DISCUSSION

In our previous [34] and present works we have investigated the influence of l on the MED characteristics for five reactions that result in the following compound nuclei: ^{244}Cm ($E^* = 77$ MeV, $T = 1.9$ MeV; and $T = 2$ MeV, $T = 3.1$ MeV—see explanations further in this paragraph), ^{224}Th ($E^* = 184$ MeV, $T = 3.1$ MeV), ^{195}Hg ($E^* = 75.7$ MeV, $T = 2$ MeV), ^{184}Pt ($E^* = 117.3$ MeV, $T = 2.65$ MeV; and $T = 2$ MeV, $T = 3.1$ MeV), and ^{162}Yb ($E^* = 117.5$ MeV, $T = 2.67$ MeV; and $T = 2$ MeV, $T = 3.1$ MeV). The initial excitation energies and the temperatures for the respective nuclei are presented in the brackets above. The first two compound systems represent the region of heavy fissioning nuclei, ^{195}Hg and ^{184}Pt are the medium fissioning nuclei, and the last one (^{162}Yb) is an example of the light fissioning nucleus. The obtained results for these three regions of the mass number A are presented in this section. To estimate the influence of l and T of compound nucleus on the MED characteristics we have carried out additional calculations for three nuclei (^{244}Cm, ^{184}Pt, and ^{162}Yb). To investigate the influence of the angular momentum on the MED parameters we performed Langevin calculations for these three nuclei with initial temperatures $T = 2$ and 3.1 MeV. The angular momentum was varied in the range $0 \div 70$. Results of these calculations have shown that the coefficients $d\langle E_K \rangle/dl^2$, $d\sigma^2_{E_K}/dl^2$, and $d\sigma^2_M/dl^2$ slightly depend on initial temperature.

A. Two-dimensional mass-energy distributions

It is known from the base of statistical theory that the variances of the mass and energy distributions increase when the temperature grows. This can be illustrated by the typical result of our calculations shown in Fig. 2.

Figure 2 contains the mass-energy distributions for ^{184}Pt and ^{244}Cm compound nuclei obtained with the fixed initial temperature $T_{\rm init}$ and angular momentum l. It is obvious from the two maps obtained for ^{244}Cm nucleus at different temperatures and $l = 70$ [Figs. 2(e) and 2(f)] that the increase of the temperature makes the MED wider both along the mass and energy axes. The influence of angular momentum on the MED for the ^{184}Pt compound is demonstrated on three upper parts of Figs. 2(a), 2(b), and 2(c). The MED changes slightly while l grows from 0 to 30. Further growth of l from 30 to 70 makes the MED much wider. We observed the same behavior for the ^{244}Cm [Figs. 2(d) and 2(e)], except for the fact that there is no angular momentum range, where the MED is practically independent of l. To make a quantitative comparison, one should analyze the one-dimensional mass and energy distributions of fission fragments. This can be done integrating the two-dimensional MED $Y(M, E_K)$ over the corresponding parameter (the kinetic energy E_K for the mass distribution or the fragment mass M for the energy distribution).

B. Angular momentum dependence of the first and the second moments of fission-fragment mass-energy distribution

The first moment of the mass distribution is the average fission-fragment mass. Prescission particle evaporation determines the mass number of the nucleus just before the split and the mass-asymmetry parameter of the nucleus at the scission point $\alpha_{\rm sc}$ specifies the mass numbers for the fission fragments. As already mentioned, for the case of hot nuclei the symmetric fission channel prevails, i.e., compound nuclei predominantly split into two equal fission fragments. This physical picture is independent of l.

A constancy of the fission-fragment mean kinetic energy $\langle E_K \rangle$ at different l and initial excitation energy was pointed out in experimental works [17,19]. The $\langle E_K \rangle$ independence of l and E^* was clarified in Refs. [17,19] with the help of experimental data on the mean γ quanta emitted from the fission fragments themselves in the reactions induced by the light charged particles and heavy ions (see the references in Ref. [19]). These investigations showed that the mean γ-quanta multiplicity M_γ and the mean γ-quanta energy increase, with the increase of E^* and l. This increase compensates the growth of rotational energy for the light fissioning nuclei at the saddle point and for the heavy ones at the scission point. Hence, authors of Refs. [17,19] drew a conclusion that the most part of the rotational energy of the fissioning nucleus transfers to the angular momenta of the fission fragments (spin) and releases further through the

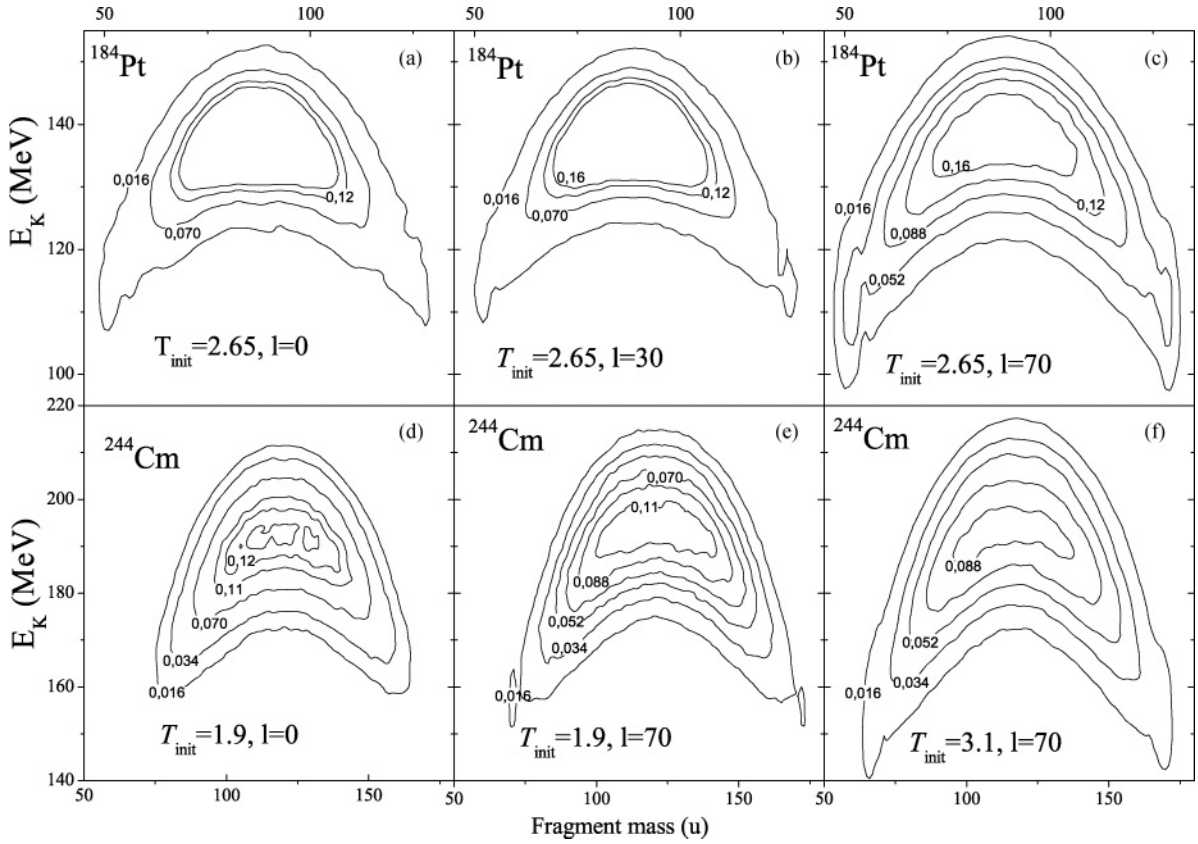

FIG. 2. Theoretical MED of fission fragments for ^{184}Pt at $T_{\rm init} = 2.65$ MeV and $l = 0$, 30, and 70 [(a), (b), (c)] and for ^{244}Cm [(d), (e), and (f)] at $T_{\rm init} = 1.9$ and 3.1 MeV and $l = 0$ and 70. The numbers at the contour lines indicate the yield in percentages, which is normalized to 200%.

γ-quanta emission from the fission fragments. They estimated the upper limit of the dependence $d\langle E_K\rangle/dl^2 \leqslant 0.3$ keV.

Our results of the $\langle E_K\rangle$ calculations for the compound nuclei ^{244}Cm, ^{184}Pt, and ^{162}Yb at two different values of the initial temperature are presented in Fig. 3. It is evident

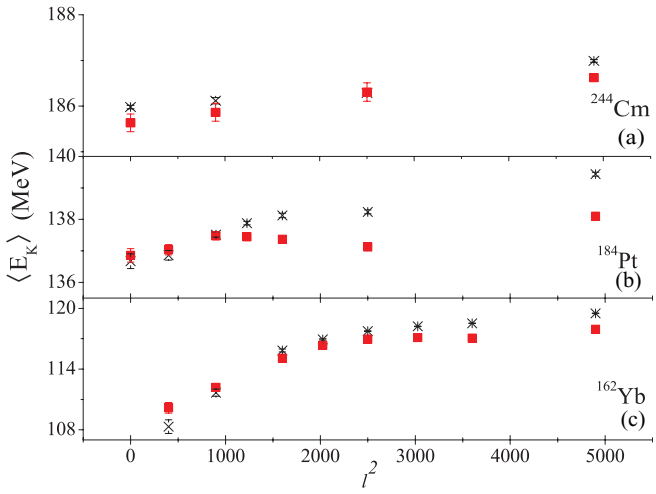

FIG. 3. (Color online) The mean total kinetic energy $\langle E_K\rangle$ as a function of l^2 for the compound nuclei ^{244}Cm (a), ^{184}Pt (b), and ^{162}Yb (c). The crosses are the $\langle E_K\rangle$ values at $T_{\rm init} = 2$ MeV and squares at $T_{\rm init} = 3.1$ MeV.

that the dependence of $\langle E_K\rangle$ on the initial excitation energy and angular momentum is weak. Our upper estimation is $d\langle E_K\rangle/dl^2 \leqslant 0.5$ keV for the heavy and medium fissioning nuclei, which is in a good agreement with the experimental one [17,19]: $d\langle E_K\rangle/dl^2 \leqslant 0.3$ keV. For the ^{162}Yb compound nucleus our estimation is much higher ($d\langle E_K\rangle/dl^2 \simeq 13.8$ keV), but there are no experimental data on $d\langle E_K\rangle/dl^2$ for this compound nucleus.

In our calculations the absolute value $|d\langle E_K\rangle/dE^*|$ does not exceed the value of 0.024, which is the maximum value for the nucleus ^{162}Yb at $l = 0$. The absolute value $|d\langle E_K\rangle/dE^*|$ is lower than 0.017 if one will analyze only medium and heavy fissioning nuclei. This value is very close to the upper estimation of the $d\langle E_K\rangle/dE^* = 0.01 \div 0.02$ found in experimental works [17,18].

The results of our calculations for variances of the mass and energy distributions are presented in Fig. 4. The top (a) and the bottom (b) graphs on this figure can be treated as the resulting graphs, where the coefficients $d\sigma_M^2/dl^2$ and $d\sigma_{E_K}^2/dl^2$ are shown together with the results of the experimental analysis [18,61] and previous theoretical results obtained within the Fokker-Planck equation. For the ^{184}Pt and ^{162}Yb nuclei the coefficients $d\sigma_M^2/dl^2$ and $d\sigma_{E_K}^2/dl^2$ change quite a bit with l. Therefore, we estimated the values of the $d\sigma_M^2/dl^2$ and $d\sigma_{E_K}^2/dl^2$ for the ranges where σ_M^2 and $\sigma_{E_K}^2$ monotonously depend on l for each nucleus. That is why there are three

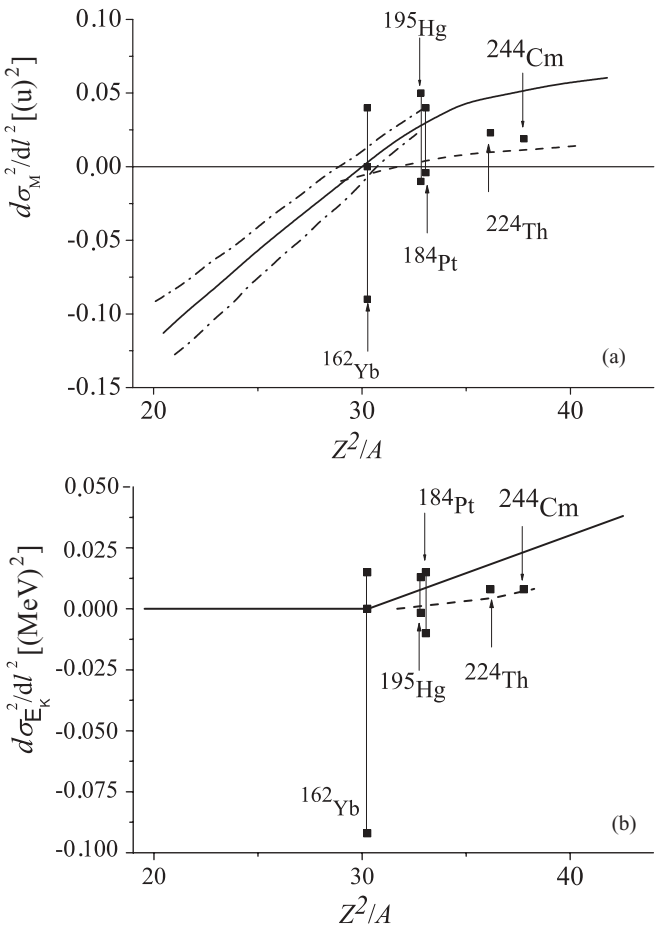

FIG. 4. The dependencies of the variance of the mass (a) and energy (b) distributions on l^2 for ^{244}Cm, ^{224}Th, ^{184}Pt, ^{195}Pt, and ^{162}Yb nuclei. The linear approximations of $d\sigma_M^2/dl^2$ and $d\sigma_{E_K}^2/dl^2$ coefficients for the investigated nuclei are plotted against Z^2/A. The solid curve and the dash-dotted curves are the results and error boundaries for the $d\sigma_M^2/dl^2$ and $d\sigma_{E_K}^2/dl^2$ coefficients from the analysis based on the experimental data [18]. The dash curve are the results of the theoretical calculations by means of the Fokker-Planck equation [23]. Solid squares are our calculated results. Two values for the ^{184}Pt, ^{195}Hg and three values for the ^{162}Yb nuclei represent the change in dependences of σ_M^2 and $\sigma_{E_K}^2$ on l. See text for details.

points for ^{162}Yb and two points for ^{184}Pt and ^{195}Hg in Fig. 4.

The coefficients $d\sigma_M^2/dl^2$ and $d\langle E_K\rangle/dl^2$ depend slightly on the initial temperature (initial excitation energy) of the nucleus and the variation of the $d\sigma_M^2/dl^2$ and $d\langle E_K\rangle/dl^2$ do not exceed 1% for the $T_{\rm init} = 2 \div 3$ MeV. The $d\sigma_{E_K}^2/dl^2$ more noticeably depends on the initial temperature and varies in the range 20–30% for the $T_{\rm init} = 2 \div 3$ MeV.

One cannot explain the dependence of σ_M^2 on l^2 considering the stiffness of the nucleus with respect to the mass asymmetry at the saddle or scision point ($d^2V/d\alpha^2$) as a function of angular momentum [34], as it was proposed on the basis of the experimental results in [17–19]. It was shown [34] that in the case of the Langevin simulations the stiffness of the nucleus along the mean Langevin trajectory is independent of l, i.e., for any given l we get the same values of the stiffness at saddle, scission, or any other point along the mean trajectory. Therefore we cannot explain obtained dependencies in the same way as the authors of Refs. [17–19], because the stiffness along the mean fission trajectory is weakly dependent on the angular momentum in the case of our dynamical modeling. The value of the "averaged" or "effective" stiffness along the descent is also independent of l. Thus, we should include additional factors into our analysis to understand the angular momentum dependence of the mass and energy variances.

The variance of the mass distribution can be estimated in the framework of the statistical approach using the following relation [61]:

$$\sigma_{M\,\rm st}^2 = A^2\,\langle T_{\rm sc}\rangle\,/16(d^2V/d\eta^2)|_{q_{\rm sc}}, \qquad (17)$$

where $\eta = 2(M_R - M_L)/(M_R + M_L)$. As long as we consider the heated nucleus, which is the thermodynamic system we should use some thermodynamic potential instead of the potential energy V. In other words, one can calculate the stiffness values as $d^2F/d\eta^2$, and Eq. (17) will be

$$\sigma_{M\,\rm st}^2 = A^2\,\langle T_{\rm sc}\rangle\,/16(d^2F/d\eta^2)|_{(q_{\rm sc},T_{\rm sc})}. \qquad (18)$$

It is evident from this relation that the temperature can also be an important factor. We should note here that the ratio $\sigma_{M\,\rm dyn}^2/\sigma_{M\,\rm st}^2$ is weakly dependent on l. This ratio is shown in Fig. 5 for different nuclei. One can see that in the case of heavy nuclei this ratio is large (about 2.8 for the ^{244}Cm nucleus). This fact demonstrates that the nucleus effectively "remembers" the descent from the saddle to the scission and "remembers" lower values of $d^2F/d\eta^2$ near the saddle point at the moment of scission. As stated above, values of $d^2F/d\eta^2$ are independent of l. Therefore, the ratio $\sigma_{M\,\rm dyn}^2/\sigma_{M\,\rm st}^2$ is independent of l for heavy and medium nuclei. One should not be confused by the evident decrease of the $\sigma_{M\,\rm dyn}^2/\sigma_{M\,\rm st}^2$ ratio for the ^{162}Yb nucleus with the increase of l. This is not caused by the angular momentum dependence of the stiffness value. As it was stated above and shown in Ref. [34] the stiffness is independent of l.

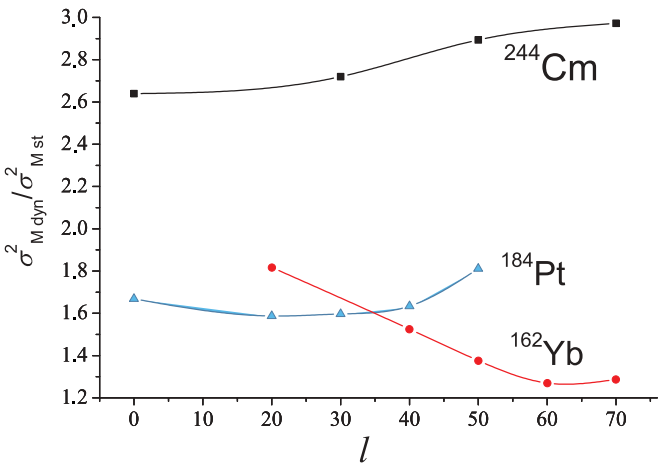

FIG. 5. (Color online) The angular momentum dependence of the ratio $\sigma_{M\,\rm dyn}^2/\sigma_{M\,\rm stat}^2$, where $\sigma_{M\,\rm dyn}^2$ is the variance of mass distribution obtained from dynamical calculations, whereas $\sigma_{M\,\rm stat}^2$ is the "statistical limit" of the variances calculated using Eq. (18) and the values of the stiffness and the temperature at the scission point.

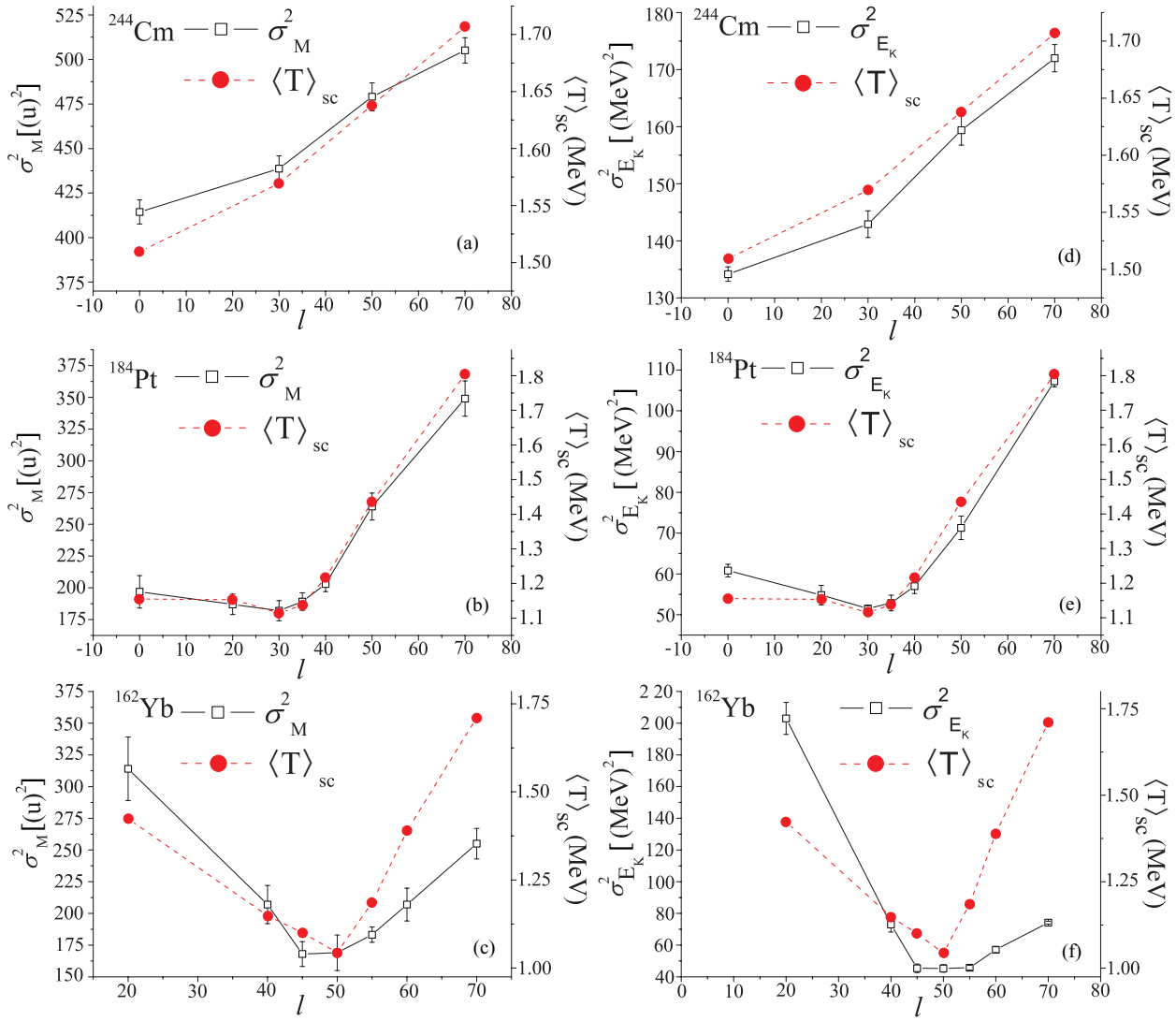

FIG. 6. (Color online) The variance of the mass [(a), (b), and (c)] and energy [(d), (e), and (f)] distributions (open squares) and the mean temperatures at the scission point (circles) for the ^{244}Cm, ^{184}Pt, and ^{162}Yb nuclei as functions of the angular momentum.

The strong decrease of $\sigma^2_{M\,\mathrm{dyn}}/\sigma^2_{M\,\mathrm{st}}$ is caused by the decrease of $\langle T_{\mathrm{sc}}\rangle$. Thus, from the results presented in Fig. 5 we can conclude that the "remembering effect" takes place especially for the heavy and the medium nuclei, but it does not cause the angular momentum dependence of σ^2_M.

Thus, other factors are coming foreground. The evaporation of the light particles changes the internal energy (or the temperature) of the nucleus. One can see from relation (18) that $\langle T_{\mathrm{sc}}\rangle$ and its dependence on l is very important for our analysis. It was explicitly demonstrated in our previous work [34] that the dependence of $\langle T_{\mathrm{sc}}\rangle$ on l follows the dependence of the σ^2_M on l. This is also well demonstrated in Fig. 6. The temperature and the variance decrease in the same range of the angular momentum values. If the temperature at the scission point is practically constant and independent of l, then the variance is weakly dependent on l. On the contrary, if the $\langle T_{\mathrm{sc}}\rangle$ depends on l, then σ^2_M will also strongly depends on l, as it could be seen Fig. 6. This figure represents also three graphs [Figs. 6(d), 6(e), and 6(f)] in the right column with the similar correlation between $\sigma^2_{E_K}$ and l.

We can generalize our conclusion that the dependences of the variances of the mass and energy distributions on l follow the dependence of $\langle T_{\mathrm{sc}}\rangle$ on the angular momentum. As a result the dependence of $\langle T_{\mathrm{sc}}\rangle$ on l cause the dependence of the variances of the mass and energy distributions on the angular momentum. The so-called remembering effect determines the "magnitude" of the variances and does not explain the dependences of σ^2_M and $\sigma^2_{E_K}$ on l.

The temperature at scission, in turn, is determined by the mean prescission neutron multiplicity $\langle n\rangle$. The more neutrons are evaporated, the colder the nucleus will be at the scission point. The detailed analysis of the dependence of $\langle T_{\mathrm{sc}}\rangle$ on the angular momentum was done in Ref. [34]. It was shown that the observed dependence of the mean scission temperature on l can be described in terms of competition between the neutron emission and fission channels of decay. It was also shown

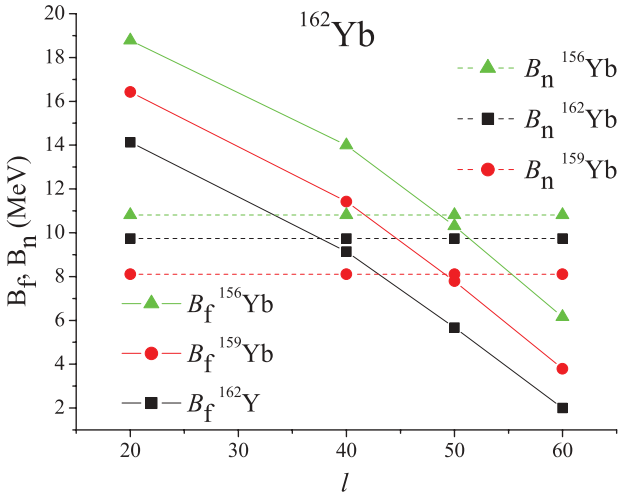

FIG. 7. (Color online) The fission barriers B_f (the solid lines) and neutron binding energies B_n (the dash lines) as functions of the angular momentum for the Yb isotopes: the lines with the squares correspond to the ^{162}Yb nucleus, the lines with the circles to ^{159}Yb, and with the triangles to ^{156}Yb.

that the obtained dependence of the mean prescission neutron multiplicity on l can be explained if one considers the ratio of the fission and neutron emission decay widths as a function of l [34].

The dependence of the neutron multiplicity on the angular momentum can be clarified using the dependences of the fission barriers (B_f) and the neutron binding energies (B_n) on l. The neutron binding energy is independent of the angular momentum value. In contrast, the value of the fission barrier is very sensitive to l. One can see from Fig. 7 that the whole investigated scope of l can be divided into the three intervals: first, where $B_n > B_f$; second, with $B_n \simeq B_f$; and, third, where $B_n < B_f$. As a result the neutron (Γ_n) and the fission (Γ_f) widths will follow to the dependences of B_n and B_f on l. For Γ_n and Γ_f we can also divide the scope of l into the three ranges, with the same bounds as it was observed for the fission barriers and the neutron binding energies.

To illustrate this the Γ_n and Γ_f are presented in Fig. 8 for the nuclei ^{156,159,162}Yb in the neutron evaporation cascade of ^{162}Yb at $T_{\text{init}} = 2.67$ MeV. The fission width $\Gamma_f \ll \Gamma_n$ and the decay time is mainly determined by the neutron width for $l < 45$. The fission probability is determined by the ratio Γ_f/Γ_n at each step of the evaporation cascade. This ratio increases as the angular momentum increases for all compound nuclei investigated in the present work. As a result, the fission probability increases steadily in comparison with the nonrotating nucleus. Another effect, which influence the ratio Γ_f/Γ_n (or fission probability) is the neutron evaporation cascade, which increases the fission probability for the system with low l and internal energy. In contrast, for $l > 55$ $B_f < B_n$ (see Fig. 7) and decay time is determined mainly by the fission width. The higher the angular momentum is, the lower B_f will be. Hence, the probability for the nucleus to evaporate many neutrons before scission becomes smaller and smaller. As a result, the number of the evaporated neutrons decreases with

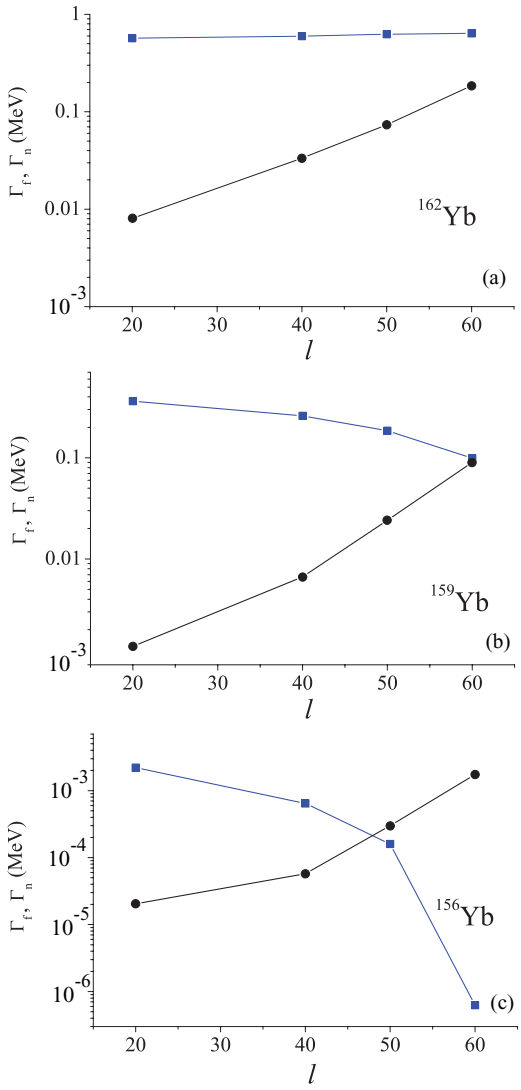

FIG. 8. (Color online) The neutron Γ_n (squares) and the fission Γ_f (circles) widths as functions of the angular momentum in the neutron evaporation cascade of the initial ^{162}Yb compound nucleus.

the increase of angular momentum. The nucleus undergoes fission more and more quickly without evaporation of large number of neutrons.

The values of B_n and B_f get closer for the intermediate values of angular momentum $45 < l < 55$. The neutron and fission widths are also close to each other. Dependence of the $\langle T_{\text{sc}} \rangle$ on the angular momentum changes in this range of l. The $\langle T_{\text{sc}} \rangle$ decreases, due to neutron evaporation increase for $l < 45$. In contrast, for $l > 50$ $B_f < B_n$ and the nuclei undergoes fission more quickly with evaporation of small number of neutrons. As a result $\langle T_{\text{sc}} \rangle$ increases.

C. Anisotropy of the fission-fragment angular distribution

In the present article the standard transitional state model [35,62,63] was used to analyze the fission-fragment angular distribution. The essence of this model consists in the assumption that there is a certain chosen (transition) configuration of

a fissile system that determines the angular distribution of the fission fragments. Thus, there are two limiting assumptions on the position of the transition state and, correspondingly, two variants of the transition-state model: the SPTS model [35,62,63] and the SCTS model [36,64,65]. It is assumed that the equilibrium distribution on the K degree of freedom (K is the projection of the compound nucleus spin I onto the symmetry axis) is established at the transition state that is usually assumed to be the saddle point. In the case of the multidimensional model, a set of the relevant conditional saddle points play the role of the transition states.

The classical SPTS model uses the following assumptions: (i) The mean time of stay of a nucleus in the saddle-point region is sufficiently larger than a characteristic time of equilibration of K mode. In other words, the time τ_{gs} of the motion of the system from the ground state to the saddle point is much longer than the relaxation time of the K degree of freedom ($\tau_{gs} \gg \tau_K$). (ii) The mean time τ_{ss} of descent of a nucleus from the saddle to scission is short in comparison with τ_K. In this case, the K distribution is formed at the saddle point and stays approximately the same. (iii) The K distribution is determined by the factor $\exp(-E_{rot}/T)$ [63].

A frequently used approximation of the fission-fragment angular distribution reads as follows:

$$W(\theta, I) = \frac{(2I+1)\exp(-p\sin^2\theta)J_0(-p\sin^2\theta)}{\mathrm{erf}\,(\sqrt{2p})}, \qquad (19)$$

where J_0 is the zeroth-order Bessel function, $p = (I + 1/2)^2/(4K_0^2)$, and the variance of the equilibrium K distribution K_0 is

$$K_0^2 = \frac{T}{\hbar^2} J_{\mathrm{eff}}, \quad J_{\mathrm{eff}} = \frac{J_\parallel J_\perp}{J_\perp - J_\parallel}. \qquad (20)$$

Here T, $J_{||}$, and $J_\perp$ are the nuclear temperature and the parallel and perpendicular moments of inertia taken at the transition state. Equation (19) is known as the Halpern-Strutinsky formula [35,63], if one will consider the saddle point as a transition state.

An average angular distribution is obtained by averaging the expression (19) over the ensemble of stochastic trajectories. The anisotropy of the fission fragment angular distribution is given by

$$A = \frac{\langle W(0^0)\rangle}{\langle W(90^0)\rangle}. \qquad (21)$$

There are three factors that determine the angular distribution: the initial spin distribution of compound nuclei, the effective inertia moments, and the nuclear temperatures at the transition states.

In the case $p \gg 1$ the anisotropy of the angular distribution is given by the approximate relation

$$\frac{\langle W(0^0)\rangle}{\langle W(90^0)\rangle} \simeq 1 + \frac{\langle I^2\rangle}{4K_0^2}. \qquad (22)$$

Equation (22) could be used for qualitative analysis of the anisotropy of angular distribution. Equation (19) is used for quantitative analysis in the present article.

The expression similar to Eq. (19) could be applied in the SCTS model, but factors determined by Eq. (20) should be calculated at the scission point, i.e., it is assumed that τ_K is much shorter than the descent time from the saddle to the scission point. In this case the equilibration of the K degree of freedom supposed to be at the scission point.

D. The effect of model dimension on the angular distribution

The set of all the accessible transition states is determined by the potential energy landscape and, hence, by the number of collective coordinates. At the same time, the particular ensemble of transition points strongly depends on the fission dynamics and, consequently, is sensitive to all the components of the model used: the conservative force, the friction and mass tensors, and so on. For instance, in the case of the SPTS model in the one-dimensional case there is only one transition state, the saddle point, for each angular momentum, whereas in the multidimensional case the entire ensemble of conditional saddle points forms the set of transition states. The multidimensional dynamic models, in comparison with the one-dimensional ones, take into account the multidimensional nature of the fission barrier. This circumstance can strongly influence the anisotropy of angular distribution predicted by models with a different number of collective coordinates involved.

In Ref. [28], we assumed that the model dimension influences the calculated angular distribution anisotropy. In addition, this influence should be stronger with increase of the nuclear fissility and excitation energy. In fact, under these conditions, the fission barrier becomes lower and a number of transition states accessible for a fissile nucleus becomes larger. An increase of the nuclear excitation energy also results in an increase of the accessible phase space to a nucleus at the ridge.

The one-dimensional Langevin equations was applied to explore the main features of angular distribution [66,67]. Recently Jia and Bao [30] published the results of the angular distribution calculations within two-dimensional Langevin dynamics. Their results are in good agreement with the experimental data. The results of the one-dimensional Langevin model are in agreement only at low excitation energies [30].

To investigate the dependence of the calculated angular distribution of fission fragments on the number of collective coordinates involved in dynamical consideration in more detail, we calculated the angular distribution anisotropy in the one-dimensional and three-dimensional Langevin models for two reactions: $^{16}\mathrm{O} + ^{208}\mathrm{Pb} \rightarrow ^{224}\mathrm{Th}$ and $^{16}\mathrm{O} + ^{232}\mathrm{Th} \rightarrow ^{248}\mathrm{Cf}$. We disregarded particle evaporation to study only dependence of the anisotropy of the angular distribution on dimensionality. Figure 9 shows that although the anisotropy of the angular distribution almost coincides in the one-dimensional and three-dimensional calculations at low excitation energies, the three-dimensional model predicts considerably higher values than the one-dimensional model at high excitation energy. It can be seen that the anisotropy of the angular distribution obtained in the three-dimensional calculations for the ^{224}Th nucleus at $E^* \simeq 150$ MeV is 30% higher than that obtained in the one-dimensional calculations. For

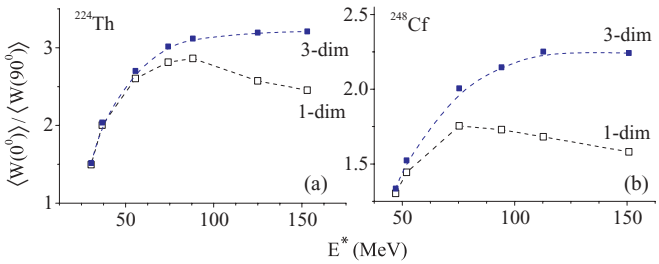

FIG. 9. (Color online) The anisotropy of the angular distribution obtained in one-dimensional (open squares) and three-dimensional (squares) Langevin calculations for the one-body mechanism of nuclear viscosity with the reduction coefficient equal to 0.25 for ^{224}Th (a) and ^{248}Cf (b) nuclei.

the nucleus ^{248}Cf this difference reaches almost 40%. Such dependence agrees with the assumption that the influence of model dimensionality should be stronger for heavier nuclei.

One should consider J_{eff} at the saddle point and its dependence on c, h, and α coordinates to explain the dependence of A on dimensionality. The saddle point is located at $h \simeq 0$ and $\alpha = 0$. A weak dependence of the effective moment of inertia on the mass-asymmetry parameter and a stronger dependence on the parameter h takes place. In this case, the values of J_{eff} decrease if the parameter h deviates from zero either on the positive or the negative sides. In the multidimensional model the anisotropy of angular distribution is calculated by averaging over the ensemble of transition points, whereas in the one-dimensional model, only one transition state (the saddle point) is realized. Therefore, the values of K_0 obtained in the three-dimensional calculations are lower on average than in the one-dimensional case due to both an increase in the effective moment of inertia and a decrease in the transition-state temperature. Lower values of the parameter K_0 correspond to a narrower angular distribution.

E. Energy dependence of the anisotropy of the angular distribution

In Fig. 10 the calculated results for the anisotropy of the angular distribution are presented for the reactions $^{16}\text{O} + ^{208}\text{Pb} \rightarrow ^{224}\text{Th}$, $^{16}\text{O} + ^{232}\text{Th} \rightarrow ^{248}\text{Cf}$, $^{16}\text{O} + ^{238}\text{U} \rightarrow ^{254}\text{Fm}$, and $^{16}\text{O} + ^{248}\text{Cf} \rightarrow ^{264}\text{Rf}$. The solid and dashed curves show the results predicted by the SPTS and SCTS models, respectively. The experimental data (open squares) are taken from Ref. [68]. It is known [35,69,70] that the SPTS model provides good reproduction of the experimental data on the anisotropy of the angular distributions for reactions where ^{3}He, α particles are used as projectiles. The compound nuclei formed in such reactions have a temperature of about 1 MeV and low angular momenta. It was found that the standard SPTS model regularly predicted low values of the angular distribution anisotropy for reaction with massive ions of carbon, oxygen, and heavy ions [69], in comparison with the experimental data, and the values obtained according to the SCTS model.

It is seen from the figure that the experimental data on the anisotropy of the fission fragment angular distribution

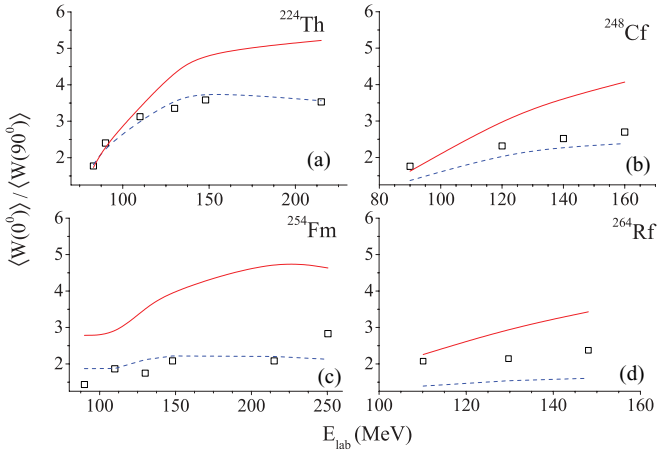

FIG. 10. (Color online) The anisotropy of the angular distribution for the compound systems ^{224}Th (a), ^{248}Cf (b), ^{254}Fm (c), and ^{264}Rf (d). The solid and dashed curves present the results predicted by the SPTS and SCTS models, respectively. The experimental data (open squares) are taken from Ref. [68].

cannot be reproduced neither of the SPTS or SCTS models especially for compound nuclei heavier than ^{224}Th and for high excitation energies. Experimental data are between the predictions of the both transition-state models [69,70]. For the case of the light compound nuclei (see results for ^{224}Th), experimental data are reproduced rather well by the SPTS model.

It was assumed [69,70] that the transition state determining the angular distribution of fission fragments could be located somewhere between the saddle point and the scission point. The existent uncertainty with the position of the transition state indicates that it is necessary to take into account the dynamical features of the angular distribution formation. In this case, the tilting mode could be considered as an independent collective coordinate in the multidimensional Langevin approach. Such completely dynamical approach makes it possible to determine, in the most general form, the nonequilibrium K-mode distribution $P(K, t)$. However, in this case, the problem of calculating the conservative force and the transport parameters (inertial and friction) for the tilting mode arises. At the same time there is no theoretical approach for calculating the transport coefficients for the tilting mode. The calculation of the transport coefficients is one of the involved problems in nuclear dynamics. Therefore, a fully dynamical consideration of the evolution of the K degree of freedom is still difficult.

The dynamical aspects of the angular distribution formation can be evaluated using the relaxation time τ_K for the tilting mode. In Refs. [71–73], it was proposed that the evolution of the tilting mode can be considered using the Monte Carlo method. In Refs. [71,72] the dynamical treatment of the tilting mode was joined with one-dimensional Langevin dynamics for shape degree of freedom, whereas three-dimensional Langevin equations for shape degree of freedom were employed in Refs. [73,74]. The K equilibration time is deduced to be $(20–30) \times 10^{-21}$ s in Refs. [71,72] and $(2–4) \times 10^{-21}$ s in Refs. [73,74] from fits of the calculated values to experimental

data on the anisotropy of the angular distribution for heavy fissioning compound systems.

Theoretical estimates of the relaxation time for the K mode and for other rotational modes in deep-inelastic-transfer reactions were obtained in Refs. [75,76], where use of the ideas of nucleon-transport theory in nuclear collisions with allowance for quantum effects [77] was made. In Refs. [75,76], the relaxation time τ_K for the tilting mode was estimated in the limits at (2–20) $\times 10^{-21}$ s, the specific value being dependent on the total angular momentum of the system.

The energy dependence of the anisotropy revealed from the developed approach [73,74] was found to be closer to the experimental data than the predictions of the statistical models SPTS and SCTS. Such phenomenologically estimated values for τ_K are comparable with the mean time of the descent from the saddle point to scission [73]. This fact points out that K-distribution changes during the descent from the saddle point to scission. These first attempts of using the Langevin dynamics joined with the Monte Carlo algorithm that considers the tilting mode as an independent collective degree of freedom seem to be promising.

IV. SUMMARY AND CONCLUSION

A stochastic approach to fission dynamics based on three-dimensional Langevin equation was applied to calculate the mass-energy and angular distributions of fission fragments formed in fission of excited compound nuclei. The angular dependence of the mass-energy distribution parameters and energy dependence of the anisotropy of the angular distribution were investigated for a wide range of fissility parameter. Analysis of the l dependence of the mass and energy distributions and anisotropy of the angular distribution performed with the statistical model indicates that it is necessary to take into account the dynamical features of the fission-fragment distributions formation. This can be done within the stochastic approach based on the Langevin equations.

The temperature-dependent FRLDM, which takes into account a diffuse nuclear surface is used in consistent way to calculate the functional of the Helmholtz free energy and level-density parameter. This model allows us to calculate consistently the fission barriers, the conservative part of the driving force, and the nuclear temperature. Thus, the temperature-dependent FRLDM allows one to determine within the same model assumptions a set of parameters, which are of special importance in statistical and dynamical simulations.

It should be stressed that the present results are the first three-dimensional full-scale work in the framework of the Langevin dynamics that aims at the question of the angular momentum and excitation energy dependence of the fission-fragment MED and $\langle E_K \rangle$, $\sigma^2_{E_K}$, and σ^2_M. We have found the following sensetivity of $\langle E_K \rangle$ on l and E^*: $|\langle E_K \rangle / dl| \leqslant 0.5$ keV and $|d\langle E_K \rangle / dE^*| \leqslant 0.017$. Both estimations are in a good agreement with experimental data [17,18].

For the coefficients $d\sigma^2_M/dl^2$ and $d\sigma^2_{E_K}/dl^2$ it was found that they are the functions of the angular momentum. Results can be summarized as follows:

(i) for the heavy fissioning nuclei (^{244}Cm and ^{224}Th) $d\sigma^2_M/dl^2 (d\sigma^2_{E_K}/dl^2) > 0$;

(ii) for the medium fissioning nuclei (^{184}Pt and ^{195}Hg) $d\sigma^2_M/dl^2 (d\sigma^2_{E_K}/dl^2) \simeq 0$ at the angular momentum $l = 0 \div 35$ and $l = 0 \div 40$, respectively, and $d\sigma^2_M/dl^2 (d\sigma^2_{E_K}/dl^2) > 0$ for $l > 35$ and $l > 40$, respectively;

(iii) for the light fissioning nucleus (^{162}Yb) $d\sigma^2_M/dl^2 (d\sigma^2_{E_K}/dl^2) < 0$ at $l = 0 \div 45$, $d\sigma^2_M/dl^2 (d\sigma^2_{E_K}/dl^2) \simeq 0$ at $l = 45 \div 50$ and $d\sigma^2_M/dl^2 (d\sigma^2_{E_K}/dl^2) > 0$ for $l > 50$.

The coefficient $d\sigma^2_M/dl^2$ is weakly dependent on the initial temperature 2 MeV $< T_{\text{init}} <$ 3 MeV (or initial excitation energy) of the nucleus. The coefficient $d\sigma^2_{E_K}/dl^2$ varies in the range of 20–30% in the investigated excitation energy range.

Our analysis shows that the obtained angular momentum dependence of σ^2_M and $\sigma^2_{E_K}$ can be clarified using the dependence of $\langle T_{\text{sc}} \rangle$ on l. The l dependence of the variances is caused by the dependence of $\langle T_{\text{sc}} \rangle$ on the angular momentum, whereas the so-called remembering effect determines the "magnitude" of the variance [34]. The temperature at scission, in turn, is determined by the mean prescission neutron multiplicity. It was shown that the observed dependence of the mean scission temperature on l can be clarified in terms of competition between neutron and fission channels of decay. The obtained dependence of the mean prescission neutron multiplicity on l can be explained if one considers the ratio of the fission and neutron decay widths as a function of l for the nuclei in the evaporation decay chain. The appropriate account for all these factors (the temperature at scission and the ratio of the fission and neutron decay widths for the fissioning nuclei in the decay chain of the initial nucleus) can be done in the dynamical model with the appropriate account of the particle evaporation.

One can conclude that the experimental data on the anisotropy of the angular distribution cannot be reproduced for the nuclei heavier than ^{224}Th and relatively high excitation energies neither within the saddle-point transition state model, nor the scission-point transition state model. The experimental data are between theoretical predictions obtained in the framework of these two models. Hence, one can suppose that for heavy nuclei at high excitation energy the so-called transition point is placed somewhere between the saddle and scission points and one should take into account the dynamical features of formation of the fission-fragment angular distribution.

ACKNOWLEDGMENTS

We thank Drs. A. Ya. Rusanov and D. O. Eremenko for enlightening and useful discussions and correspondence. The authors are grateful to U. Turlykina and Dr. R. Dreyer for a careful reading of the manuscript. One of us (P.N.N.) is grateful to the Istituto Nazionale di Fisica Nucleare (INFN) for the financing of the stay at Naples and also thanks the Naples section of INFN for the hospitality extended to him during the course of this work.

[1] A. Bohr and B. Mottelson, *Nuclear Structure* (Benjamin, New York, 1975), Vol. 2, p. 534.
[2] S. Shlomo and V. M. Kolomietz, Rep. Prog. Phys. **68**, 1 (2005).
[3] M. G. Itkis, V. N. Okolovich, A. Ya. Rusanov, and G. N. Smirenkin, Phys. Part. Nuclei **19**, 701 (1988).
[4] J. R. Nix and W. J. Swiatecki, Nucl. Phys. **A71**, 1 (1965).
[5] J. R. Nix, Nucl. Phys. **A130**, 241 (1969).
[6] F. Plasil, D. S. Burnett, H. C. Britt, and S. G. Thompson, Phys. Rev. **142**, 696 (1966).
[7] H. J. Krappe and J. R. Nix, *Proceedings of the Third IAEA Symposium on Physics and Chemistry of Fission (Rochester)* (Vienna: IAEA, 1973), Vol. 1, p. 159.
[8] H. J. Krappe, J. R. Nix, and A. J. Sierk, Phys. Rev. C **20**, 992 (1979).
[9] H. J. Krappe, J. R. Nix, and A. J. Sierk, Phys. Rev. Lett. **42**, 215 (1979).
[10] A. J. Sierk, Phys. Rev. C **33**, 2039 (1986).
[11] P. Möller and J. R. Nix, At. Data Nucl. Data Tables **39**, 213 (1988).
[12] P. Möller and J. R. Nix, J. Phys. G **20**, 1681 (1994).
[13] P. Möller, J. R. Nix, W. D. Myers, and W. J. Swiatecki, At. Data Nucl. Data Tables **59**, 185 (1995).
[14] M. Brack, C. Guet, and H. B. Håkansson, Phys. Rep. **123**, 275 (1985).
[15] H. J. Krappe, Phys. Rev. C **59**, 2640 (1999).
[16] C. Guet, E. Strumberger, and M. Brack, Phys. Lett. **B205**, 427 (1988).
[17] G. G. Chubaryan, M. G. Itkis, S. M. Lukianov *et al*., Yad. Fiz. **56**, 3 (1993) [Phys. At. Nucl. **56**, 286 (1993)].
[18] M. G. Itkis, Yu. A. Muzychka, Yu. Ts. Oganessian *et al*., Yad. Fiz. **58**, 2140 (1995) [Phys. At. Nucl. **58**, 2026 (1995)].
[19] M. G. Itkis and A. Ya. Rusanov, Phys. Part. Nuclei **29**, 389 (1998).
[20] C. Gregoire and F. Scheuter, Z. Phys. A **303**, 337 (1981).
[21] M. E. Faber, Z. Phys. A **297**, 277 (1980); M. E. Faber, Phys. Rev. C **24**, 1047 (1981).
[22] B. G. Glagola, B. B. Back, and R. R. Betts, Phys. Rev. C **29**, 486 (1984).
[23] G. D. Adeev, I. I. Gontchar, V. V. Pashkevich, N. I. Pischasov, and O. I. Serdyuk, Phys. Part. Nuclei **19**, 1229 (1988).
[24] G. D. Adeev, I. I. Gontchar, L. A. Marchenko, and N. I. Pischasov, Yad. Fiz. **43**, 1137 (1986) [Sov. J. Nucl. Phys. **43**, 727 (1986)].
[25] Y. Abe, S. Ayik, P. G. Reinhard, and E. Suraud, Phys. Rep. **275**, 49 (1996).
[26] G. D. Adeev, A. V. Karpov, P. N. Nadtochy, and D. V. Vanin, Phys. Part. Nuclei **36**, 712 (2005).
[27] A. V. Karpov, P. N. Nadtochy, D. V. Vanin, and G. D. Adeev, Phys. Rev. C **63**, 054610 (2001).
[28] P. N. Nadtochy, G. D. Adeev, and A. V. Karpov, Phys. Rev. C **65**, 064615 (2002).
[29] A. V. Karpov, P. N. Nadtochy, E. G. Ryabov, and G. D. Adeev, J. Phys. G: Nucl. Part. Phys. **29**, 2365 (2003).
[30] Y. Jia and J. D. Bao, Phys. Rev. C **75**, 034601 (2007).
[31] Y. Aritomo and M. Ohta, Nucl. Phys. **A753**, 152 (2005).
[32] N. D. Mavlitov, P. Fröbrich, and I. I. Gontchar, Z. Phys. A **342**, 195 (1992).
[33] P. Fröbrich and I. I. Gontchar, Nucl. Phys. **A563**, 326 (1993).
[34] E. G. Ryabov, A. V. Karpov, and G. D. Adeev, Nucl. Phys. **A765**, 39 (2006).
[35] R. Vandenbosh and J. R. Huizenga, *Nuclear Fission* (Academic, New York, 1973).
[36] H. H. Rossner, J. R. Huizenga, and W. U. Schröder, Phys. Rev. Lett. **53**, 38 (1984).
[37] E. G. Ryabov, and G. D. Adeev, Yad. Fiz. **68**, 1583 (2005 [Phys. At. Nucl. **68**, 1525 (2005)].
[38] M. Brack *et al*., Rev. Mod. Phys. **44**, 320 (1972).
[39] K. T. R. Davies, A. J. Sierk, and J. R. Nix, Phys. Rev. C **13**, 2385 (1976); J. R. Nix and A. J. Sierk, Nucl. Phys. **A428**, 161 (1984).
[40] J. R. Nix and A. J. Sierk, *Proceedings of the International School-Seminar on Heavy Ion Physics, Dubna, USSR, 1986*, edited by M. I. Zarubina and E. V. Ivashkevich (JINR, Dubna, 1987), p. 453; J. R. Nix, Nucl. Phys. **A502**, 609 (1989).
[41] J. R. Nix and A. J. Sierk, *Proceedings of the Sixth Adriatic Conference on Nuclear Physics: Frontiers of Heavy Ion Physics, Dubrovnik, Yugoslavia, 1987*, edited by N. Cindro, R. Caplar, and W. Greiner (World Scientific, Singapore, 1990), p. 333.
[42] P. Fröbrich and I. I. Gontchar, Phys. Rep. **292**, 131 (1998).
[43] I. I. Gontchar, L. A. Litnevsky, and P. Fröbrich, Comput. Phys. Commun. **107**, 223 (1997).
[44] J. Marten and P. Fröbrich, Nucl. Phys. **A545**, 854 (1992).
[45] P. Fröbrich, Nucl. Phys. **A787**, 170 (2007).
[46] S. G. McCalla and J. P. Lestone, Phys. Rev. Lett. **101**, 032702 (2008).
[47] V. Zagrebaev and W. Greiner, J. Phys. G **31**, 825 (2005).
[48] S. Cohen, F. Plasil, and W. J. Swiatecki, Ann. Phys. (NY) **82**, 557 (1974).
[49] K. T. R Davies and J. R. Nix, Phys. Rev. C **14**, 1977 (1976).
[50] A. V. Ignatyuk, M. G. Itkis, V. N. Okolovich, G. N. Smirenkin, and A. S. Tishin, Yad. Fiz. **21**, 1185 (1975) [Sov. J. Nucl. Phys. **21**, 612 (1975)].
[51] J. Töke and W. J. Swiatecki, Nucl. Phys. **A372**, 141 (1981).
[52] P. Fröbrich and R. Lipperheide, *Theory of Nuclear Reactions* (Clarendon Press, Oxford, 1996).
[53] R. W. Hasse and W. Stocker, Phys. Lett. **B44**, 26 (1973).
[54] M. Diebel, K. Albrecht, and R. Hasse, Nucl. Phys. **A355**, 66 (1981).
[55] T. Wada, Y. Abe, and N. Carjan, Phys. Rev. Lett. **70**, 3538 (1993).
[56] X. Campi and S. Stringari, Z. Phys. A **309**, 239 (1983).
[57] K. T. R. Davies, R. A. Managan, J. R. Nix, and A. J. Sierk, Phys. Rev. C **16**, 1890 (1977).
[58] P. N. Nadtochy and G. D. Adeev, Phys. Rev. C **72**, 054608 (2005); M. V. Borunov, P. N. Nadtochy, and G. D. Adeev, Nucl. Phys. **A799**, 56 (2008).
[59] N. Carjan and M. Kaplan, Phys. Rev. C **45**, 2185 (1992).
[60] S. J. Sanders, A. Szanto de Toledo, and C. Beck, Phys. Rep. **311**, 487 (1999).
[61] A. Ya. Rusanov, V. V. Pashkevich, and M. G. Itkis, Yad. Fiz. **62**, 595 (1999) [Phys. At. Nucl. **62**, 547 (1999)].
[62] A. Bohr, *Proceedings of the United Nations International Conference on the Peaceful Uses of Atomic Energy* (United Nations, New York, 1956), Vol. 2, p. 151.
[63] I. Halpern and V. M. Strutinsky, *Proceedings of the United Nations International Conference on the Peaceful Uses of Atomic Energy* (United Nations, Geneva, 1958), Vol. 15, p. 408.
[64] P. D. Bond, Phys. Rev. C **32**, 471 (1985); P. D. Bond, Phys. Rev. C **32**, 483 (1985).
[65] H. H. Rossner, J. R. Huizenga, and W. U. Schröder, Phys. Rev. C **33**, 560 (1986).
[66] P. Fröbrich and H. Rossner, Z. Phys. A **349**, 99 (1994).

[67] V. A. Drozdov, D. O. Eremenko, S. Yu Platonov, O. V. Fotina, and O. A. Yuminov, Yad. Fiz. **64**, 221 (2001) [Phys. At. Nucl. **46**, 179 (2001)].
[68] B. B. Back, R. R. Bets, J. E. Gindler *et al*., Phys. Rev. C, **32**, 195 (1985).
[69] L. C. Vaz and J. M. Alexander, Phys. Rep. **97**, 1 (1983); R. Freifelder, M. Prakash, and J. M. Alexander, *ibid*. **133**, 315 (1986).
[70] J. O. Newton, Phys. Part. Nuclei **21**, 821 (1990).
[71] V. A. Drozdov, D. O. Eremenko, O. V. Fotina, S. Yu Platonov, and O. A. Yuminov, *Proc. of Tours Symposium on Nuclear Physics V, 2003*, edited by M. Arnold, M. Lewitowicz, G. Münzenberg, H. Akimune, M. Ohta, H. Utsunomiya, T. Wada, and T. Yamagata (AIP, Melville, NY, 2004), Vol. 704, p. 130.
[72] D. O. Eremenko, V. A. Drozdov, M. H. Eslamizadex, O. V. Fotina, S. Yu Platonov, and O. A. Yuminov, Yad. Fiz. **69**, 1458 (2006) [Phys. At. Nucl. **69**, 1423 (2006)].
[73] A. V. Karpov, R. M. Hirjanov, A. V. Sagdeev, and G. D. Adeev, J. Phys. G: Nucl. Part. Phys. **34**, 255 (2007).
[74] R. M. Hiraynov, A. V. Karpov, and G. D. Adeev, Yad. Fiz. **71**, 1389 (2008) [Phys. At. Nucl. **71**, 1361 (2008)].
[75] T. Døssing and J. Randrup, Nucl. Phys. **A433**, 215 (1985).
[76] T. Døssing and J. Randrup, Nucl. Phys. **A475**, 557 (1987).
[77] J. Randrup, Nucl. Phys. **A327**, 490 (1979).